Calcium-responsive transactivator (CREST) toxicity is rescued by loss of PBP1/ATXN2 function in a novel yeast proteinopathy model and in transgenic flies

By Sangeun Park[1], Sei-Kyoung Park[1], Naruaki Watanabe[2], Tadafumi Hashimoto[2], Takeshi Iwatsubo[2], Tatyana A. Shelkovnikova[3] and Susan W. Liebman[1]*

1 Department of Pharmacology, U. of Nevada, Reno, USA.

2 Department of Neuropathology, U. of Tokyo, Tokyo, Japan

3 Medicines Discovery Institute, Cardiff University, Cardiff, UK

Correspondence and requests for materials should be addressed to S.W.L.

(e-mail: sliebman@unr.edu)

Short title: **A yeast model of calcium-responsive transactivator (CREST) proteinopathy**

Abstract

Proteins associated with familial neurodegenerative disease often aggregate in patients' neurons. Several such proteins, e.g. TDP-43, aggregate and are toxic when expressed in yeast. Deletion of the ATXN2 ortholog, *PBP1,* reduces yeast TDP-43 toxicity, which led to identification of ATXN2 as an amyotrophic lateral sclerosis (ALS) risk factor and therapeutic target. Likewise, new yeast neurodegenerative disease models could facilitate identification of other risk factors and targets. Mutations in *SS18L1,* encoding the calcium-responsive transactivator (CREST) chromatin-remodeling protein, are associated with ALS. We show that CREST is toxic in yeast and, like the yeast chromatin-remodeling factor SWI1, CREST inhibits silencing of *FLO* genes. Toxicity of CREST is enhanced by the [*PIN*$^+$] prion and reduced by deletion of *PBP1/ATXN2.* CREST forms nuclear and occasionally cytoplasmic foci that stain with an amyloid dye. Overexpression of PBP1 caused considerable CREST co-localization with PBP1 tagged cytoplasmic granules which might promote toxic aggregation of CREST. In accord with the yeast data, we show that the Drosophila ortholog of human ATXN2, dAtx2, is a potent enhancer of CREST toxicity. Down regulation of dAtx2 in flies overexpressing CREST in retinal ganglion cells was sufficient to almost entirely rescue the severe degenerative phenotype induced by human CREST. These results extend the spectrum of ALS associated proteins affected by *PBP1/ATXN2*, suggesting that therapies targeting ATXN2 may be effective for a wide range of neurodegenerative diseases.

Author summary

Mutations in the calcium-responsive transactivator (CREST) protein have been shown to cause amyotrophic lateral sclerosis (ALS). Here we show that the human CREST protein expressed in yeast forms nuclear aggregates and is toxic. We also show that ATXN2, previously shown to modify ALS toxicity caused by mutations in the TDP-43 encoding gene, also modifies toxicity of CREST expressed in either yeast or flies. These results extend the spectrum of ALS associated proteins affected by *ATXN2*, suggesting that therapies targeting ATXN2 may be effective for a wide range of neurodegenerative diseases.

Introduction

Mutations in an increasing number of human genes have been found to cause familial neurodegenerative disease [1,2]. Proteins encoded by these genes are often soluble in healthy individuals, but form insoluble amyloid-like aggregates that seed further aggregation in the neurons of patients with disease. For example, such conformational changes have been seen for: Aβ, associated with Alzheimer's disease; α-synuclein with Parkinson's disease; TDP-43, FUS and others with amyotrophic lateral sclerosis (ALS) and frontotemporal dementia (FTD); and huntingtin with Huntington's disease. Wild-type and mutant forms of these proteins are respectively associated with aggregates in sporadic and familial forms of the diseases. Overexpression of either wild-type or mutant protein causes toxicity, although the mutant forms are often toxic at lower concentrations than the wild-type [3].

Conformational change of several yeast proteins from a soluble state to insoluble self-seeding aggregates, called prions, causes transmissible phenotypic changes [4-15]. Furthermore, the presence of one prion aggregate enhances the *de novo* appearance of heterologous prions. For example, the endogenous yeast prion [*PIN*$^+$], which is an amyloid form of the RNQ1 protein, promotes the *de novo* aggregation of the SUP35 protein to form the [*PSI*$^+$] prion. This could occur by cross-seeding or by sequestration of proteins such as chaperones by the amyloid [*PIN*$^+$] prion [8,16-27].

Yeast has proved to be useful in the study of disease-specific proteins that form prion-like aggregates [28-35]. When human proteins associated with aggregation in neurodegenerative disease were expressed in yeast, they formed aggregates and caused toxicity. Curiously the toxicity of several of these proteins, e.g. TDP-43, FUS or huntingtin, is enhanced by the presence of the [*PIN*$^+$] prion [28,36,37]. These yeast models have allowed the identification of yeast genes that either alter the disease protein's aggregation or enhance or reduce its toxicity. Remarkably, human homologs of these yeast modifier genes have confirmed (*PICALM* for Alzheimer's [38-40], *PARK9* for Parkinson [38,41]), and identified new (*ATXN2* [42-46] for ALS and *XPO1*, *ADSSL1* and *RABGEF1* for Alzheimer's [38,40]), human risk factors for the modeled disease. Indeed, the discovery in yeast that deletion of the *ATXN2* (Ataxin-2) ortholog, *PBP1,* reduced TDP-43 toxicity, led to the recent exciting finding that

reduction in ATXN2 levels dramatically lowers neurotoxicity in ALS mouse models [43]. Thus the establishment of new yeast neurodegenerative disease models may lead to the identification of new risk factors for human disease as well as provide a screening platform for drug discovery.

Recently, mutations in *SS18L1* have been shown to cause ALS [47,48]. *SS18L1* encodes the calcium-responsive transactivator (CREST) protein which is an essential component of the nBAF neuron-specific chromatin remodeling complex that is related to the yeast SWI/SNF chromatin remodeling complex [49-51]. Overexpression of CREST inhibits neurite outgrowth in cultured neurons and causes retina degeneration in transgenic Drosophila [48,52]. Also, CREST co-immunoprecipitates with FUS in neuron lysates [48,52]. In cultured cells, transformed CREST forms predominantly nuclear dots with some cytoplasmic foci. Also, like other ALS associated proteins, CREST is recruited to stress-induced ribonucleoprotein particle (RNP) granules [52,53]. RNP proteins must reversibly aggregate in physiological granules as part of their normal cellular function, but this ability to aggregate could lead to the formation of pathological aggregates. Indeed, TDP-43 and FUS have prion-like domains and have been found in cytoplasmic aggregates in the neurons of patients with ALS. While no such patient aggregates have yet been reported for CREST, it has an unstructured prion-like domain predicted to form amyloid-like aggregates [48]. CREST in cell culture was slightly resistant to Triton-X100 but was solubilized by SDS; in addition it formed nuclear dots in a concentration-dependent manner [52].

Here we establish a new ALS model in yeast. We show that this human chromatin remodeling complex component and transcriptional activator is toxic and forms largely nuclear aggregates that stain with an amyloid dye when expressed in yeast. We also show that CREST toxicity is increased by the endogenous yeast [*PIN*$^{+}$] prion. Furthermore, like SWI1 [54], CREST inhibits telomeric and epigenetic silencing of *FLO* genes thereby enhancing flocculation (cell clumping). Deletion of the TDP-43 toxicity modifier, *PBP1,* likewise reduces CREST toxicity and this finding was also confirmed in a CREST transgenic fly model. Finally, overexpression of *PBP1*, causes a large portion of CREST to leave the nucleus and co-localize with PBP1-GFP containing cytoplasmic granules.

Results

Expression of human CREST in yeast is toxic.

Growth of yeast transformed with control *GAL-GFP* vectors was compared with yeast expressing fusions of human CREST cDNA and GFP from a *GAL* promoter on three types of vectors: a **Y**east ***C****EN* **p**lasmid (YCp) containing a centromere and expressed as one or a few copies in each cell (Fig. 1a); a **Y**east **E**pisomal **p**lasmid (Yep) containing elements of the endogenous yeast 2μ episome and expressed in high copy in some cells but absent in other cells (Fig. 1b); or a **Y**east **I**ntegrating **p**lasmid (YIp) that was integrated into the genome (Fig. 1c). Expression of the *GAL* controlled genes was turned on with a constitutively expressed fusion of the human estrogen receptor hormone-binding domain, the yeast *GAL4* DNA-binding domain and the VP16 viral transcriptional activator, which was activated by the addition of β-estradiol [55]. The high level of β-estradiol used here (1μM) in glucose media results in more expression from the *GAL* promoter than that obtained by traditional induction on 2% galactose without β-estradiol [56]. Growth inhibition is evident but slight when CREST-GFP was expressed from a *CEN* vector (Fig. 1a) and more inhibition is seen when episomal (Fig. 1b) or integrating vectors (Fig. 1c) were used.

Since the presence of the [*PIN*$^+$] prion causes enhanced toxicity of the human genes huntingtin/polyQ, TDP-43 and FUS [28,36,37,57] , we asked if [*PIN*$^+$] would likewise increase toxicity of CREST and found that it did (Fig. 2a). However, CREST and [*PIN*$^+$] aggregates did not co-localize (Fig. 2b). Also, CREST aggregated in both [*PIN*$^+$] and [*pin*$^-$] cells (Figs 2b and 2c) and was toxic (Fig. 2d) even in cells lacking the HSP104 chaperone required for the propagation of many yeast prions [4,58]. Note the reduced induction of CREST caused by galactose relative to β-estradiol results in reduced toxicity.

Expression of human CREST activates yeast *FLO* genes and causes flocculation.

While working with *GAL-CREST-GFP* and *GAL-GFP* transformants we noticed that expression of CREST-GFP caused cells in liquid culture to settle very rapidly compared to the GFP controls. In a

measured experiment we found that overexpression of CREST caused flocculation (cell clumping), while overexpression of TDP-43 or FUS did not (Fig. 3a).

Since CREST increased yeast flocculence just as the non-prion form of the SWI1 chromatin remodeling protein does [54], we hypothesized that CREST, like SWI1, remodels yeast chromatin structure causing a release of silencing of telomerically located and epigenetically controlled [59] *FLO* genes, resulting in flocculation. To test this we examined the effect of CREST on the telomerically located *FLO1* and the epigenetically controlled *FLO11* promoters, using *ura3Δ* strains with either the *FLO1* or *FLO11* open reading frames (ORFs) replaced with the *URA3* ORF reporter [54]. In the absence of CREST these strains were auxotrophic for uracil indicating that both the *FLO1* and *FLO11* promoters were off. However, upon CREST expression on galactose medium, both strains gained the ability to grow in the absence of uracil, indicating that the *FLO1* and *FLO11* promoters were indeed both activated by CREST (Fig. 3b).

CREST forms largely nuclear and occasionally cytoplasmic amyloid foci.

Similar to mammalian cells [52], CREST-GFP expressed in either [*PIN*$^+$] or [*pin*$^-$] yeast was localized to nuclear dots (Figs 4a and 5a). CREST-GFP dots were largely clustered in nuclei but smaller cytoplasmic foci were also visible especially after longer induction times (Fig. 4a). Nuclear localization was confirmed by using a constitutively expressed nuclear HTB1-mCh marker (Figs 4b and Supplementary Fig. S1) which co-localized with CREST-GFP. CREST foci also stained with the amyloid dye thioflavin T (Fig. 4c). For controls we show TDP-43 and FUS aggregates that, respectively do not and do, stain with thioflavin T[60]. In addition, the bulk of the CREST protein is found in the pellet of lysates while the non-aggregated proteins, GFP and PGK, remain in the supernatant (Fig. 4d).

When CREST was overexpressed in mammalian cells, it formed large dot-like nuclear structures and was also present in cytoplasmic aggregates [52]. When CREST is expressed in yeast for 5-6 h, most of the protein is found in nuclear dots with just occasional cytoplasmic foci (see Fig. 4 and Fig. 5 left). However, when cells with nuclear CREST are stressed by incubation at high temperature there is a dramatic increase in the appearance of cytoplasmic foci (Fig. 5 middle) that partially co-

localize with Ded1-mCh stress granule and EDC3-mCh P-body markers. Following a return to 30°C, cytoplasmic CREST aggregates disappear along with stress granules and P-bodies (Fig. 5 right).

Unlike [*PIN*$^+$] aggregates, CREST dots and foci do not seed SUP35 prion formation.

Considerable evidence suggests that amyloid-like aggregates of one protein can facilitate the *de novo* aggregation of certain heterologous proteins. Such a phenomenon could be an important risk factor for disease. While there are no yeast proteins that are homologous to the human CREST, the yeast protein with the most similarity to CREST, using a BLAST search, is RNQ1, the [*PIN*$^+$] protein. This is likely due to the extensive QN-rich regions in both proteins. Thus, we asked if aggregates of CREST, like [*PIN*$^+$] and other QN-rich aggregates, could facilitate the *de novo* aggregation of SUP35 to form the [*PSI*$^+$] prion. In [*PIN*$^+$] but not [*pin*$^-$] cells, transient overexpression of SUP35NM-GFP causes the appearance of large fluorescent SUP35NM-GFP rings and converts [*psi*$^-$] cells into [*PSI*$^+$] [8,17,56,62]. Here we detect conversion into [*PSI*$^+$], which causes readthrough of nonsense codons, by the appearance of adenine prototrophy despite the presence of the nonsense mutation *ade1-14.* We found that unlike [*PIN*$^+$], or overexpression of a variety of QN-rich yeast proteins[8], overexpression of CREST did not cause the appearance of fluorescent SUP35NM-GFP rings or of adenine prototrophy. This was true even when *PBP1* was also overexpressed to drive CREST-dsRED aggregates into the cytoplasm (Supplementary Fig. S2).

PBP1 affects the aggregation and toxicity of CREST in yeast and flies.

Overexpression of yeast's *PBP1*, a homolog of human *ATXN2*, enhances, while *PBP1* deletion reduces, the toxicity of TDP-43 expressed in yeast [42]. This led to the discovery that ATXN2 intermediate-length polyglutamine expansions, which are associated with increased ATXN2 protein levels, are a risk factor for ALS [42]. Work in a variety of model organisms including mice, now suggests that *ATXN2* is a modifier of some neurodegenerative diseases [43].

We thus tested the effect of *PBP1* level on the aggregation and toxicity of CREST in yeast. We found a dramatic increase in cytoplasmic CREST dots when *PBP1* was overexpressed Fig. 6a. This

was not due to an increase in CREST protein level (Fig. 6b). We also found the CREST-DsRed dots co-localized with PBP1-GFP cytoplasmic granules (Fig. 6c). Overexpression of *PBP1* itself was toxic in our system (Fig. 6d) so the effect on CREST toxicity could not be determined.
However, we clearly show that deletion of *PBP1* reduced toxicity in either a [*PIN*$^+$] or [*pin*$^-$] background (Fig. 6e). This was not due to either a reduced level of CREST or an increase in its solubility (Figs 6b and 4d). Also, we did not detect any effect of *pbp1Δ* on the microscopically observed cellular location of CREST-GFP.

In order to validate the observed effect of the ATXN2 homolog PBP1 in an independent *in vivo* model, we used transgenic Drosophila which possesses an ortholog of the human *ATXN2* gene, dAtx2. Overexpression of untagged CREST using GAL4-UAS system in Drosophila lines results in severe retinal degeneration [52] . For our studies, we used dAtx2 deletion fly line (dAtx2 06490) [61]. Homozygous deletion of dAtx2 was reported to cause disorganized and decreased photoreceptor neurons, but there was no effect in the heterozygous state [61]. We crossed CREST overexpressing (transgenic, TG) flies with heterozygous dAtx2 flies (dAtx2$^{06490\ /+}$) and analyzed the double TG progeny. Histological analysis confirmed normal retinal morphology in of dAtx2$^{06490\ /+}$ flies, whereas complete disruption of the regularly ordered arrays of photoreceptor neurons was observed in the retina in CRESTwt TG flies, consistent with the previous reports (Fig. 7). Strikingly, this severe retinal degenerative phenotype in CRESTwt TG flies was almost entirely rescued by downregulation of dAtx2 (CRESTwt TG; dAtx2$^{06490\ /+}$ line) (Fig. 7). Thus, human CREST toxicity in flies is largely mediated by endogenous dAtx2.

Discussion

Our data show that human CREST expressed in yeast shares properties with other ALS associated proteins: CREST and FUS form amyloid foci; CREST, TDP-43 and FUS toxicity is enhanced by the yeast prion [*PIN*$^+$]; TDP-43 and CREST toxicity is reduced by deletion of *PBP1*; CREST, TDP-43 and FUS are associated with cytoplasmic RNP granules.

We first described [*PIN*$^+$], the prion form of the RNQ1 protein, because its presence allowed the efficient conversion of the SUP35 protein to its prion form, [*PSI*$^+$] [8,17,63]. It was later shown that [*PIN*$^+$] is also required for the efficient aggregation and toxicity of polyQ in yeast [28]. The mechanisms causing these effects are still unknown. Some data support the hypothesis that the [*PIN*$^+$] aggregates of RNQ1 cross-seed aggregation of heterologous proteins such as SUP35 and polyQ. Likewise some, but not all evidence suggests that the [*PIN*$^+$] aggregates bind proteins such as chaperones that would otherwise inhibit aggregation of the heterologous SUP35 or polyQ protein, thereby enhancing their aggregation [18-25,27]

We recently showed that toxicity of TDP-43 and FUS is enhanced by the presence of [*PIN*$^+$] [37,57]. Both of these proteins contain Q/N-rich regions and co-aggregate with polyQ disease protein alleles of huntingtin [64,65]. Surprisingly, we did not detect a clear effect of [*PIN*$^+$] on TDP-43 or FUS aggregation. Likewise, CREST is a Q-rich protein. We show here that the toxicity of CREST is enhanced by [*PIN*$^+$], again with no clear effect on aggregation. Apparently the toxicity of the aggregates is altered without a change in their appearance. A recent finding that deletion of PBP1 causes a reduction in the level of RNQ1 protein [66] could have explained the reduced CREST, TDP-43 and FUS toxicity seen in *pbp1Δ* cells if the lowered RNQ1 level reduced the potency of [*PIN*$^+$]. However, we show here that this is not the case because *pbp1Δ* reduces CREST toxicity even in the absence of [*PIN*$^+$] (Fig. 6e).

We have shown that the presence of certain QN-rich aggregates can substitute for [*PIN*$^+$] and allow the efficient induction of [*PSI*$^+$] by overexpression of SUP35 [8]. This fact, plus the observation that RNQ1, the [*PIN*$^+$] prion protein, although not a homolog, is the yeast protein most similar to CREST, prompted us to ask if overexpression of CREST could substitute for [*PIN*$^+$]. However, CREST did not provide any [*PIN*$^+$] activity even when PBP1 was overexpressed driving CREST into the cytoplasm.

Prion aggregates enhance *de novo* formation of heterologous prion, presumably by a cross-seeding mechanism. Curiously, however, if heterologous prion is already present, prion aggregates instead promote loss of the heterologous prion [20]. One mechanism for this has been shown to be

prion aggregate binding to, and therefore titration of, chaperones needed to propagate the heterologous prion [24]. Likewise, CREST has been shown to suppress polyQ-mediated huntingtin aggregation and toxicity [67].

Many of the ALS associated proteins, e.g. TDP-43, FUS and TAF15 are soluble nuclear RNA/DNA binding proteins that regulate mRNA splicing and/or stability and contain prion-like unstructured domains and nuclear/cytoplasmic trafficking signals. In neurons of patients with ALS/FTD these proteins have been found in cytoplasmic aggregates instead of their normal nuclear location. This suggests that impaired nucleocytoplasmic transport may be a general mechanism for neurotoxicity [3,68-73]. Indeed, impairing nuclear import of TDP-43 enhances neurotoxicity [74].

While TDP-43 and FUS quickly form cytoplasmic aggregates in yeast with little or no nuclear localization [31,32,37,57,75-77], we found here that CREST appeared in nuclear aggregates with only occasional cytoplasmic foci. While the ALS associated proteins TDP-43, FUS and SOD1 form aggregates in patients, model systems and *in vitro*, these aggregates are sometime but not always classical amyloids. In yeast, FUS, but not TDP-43, aggregates stain with the amyloid dye thioflavin T [60]. Although both nuclear and cytoplasmic CREST foci appear to stain with thioflavin T and therefore contain amyloid, it is still tempting to speculate, by analogy with FUS and TDP-43, that the CREST cytoplasmic foci are more toxic than nuclear CREST. It is unknown if similar aggregates form in patients and associated with neuronal death.

We found that heat stress induced CREST to leave the nucleus and partially co-localize with RNP granules. This is consistent with previous findings in mammalian cells that CREST becomes mislocalized to the cytoplasm under stressful conditions (oxidative stress) and becomes recruited to cytoplasmic stress granules [52]. Furthermore, as seen for classic stress granule proteins, CREST returned to the nucleus in yeast following the heat stress. Many proteins associated with neurodegenerative disease contain intrinsically disordered regions that are required for their appearance in RNP granules. Evidence has been accumulating that RNP granules are incubators for the formation of pathogenic protein aggregates associated with neurodegenerative disease. It has been proposed that localization of proteins such as TDP-43, FUS and C9OFR72-encoded dipeptide repeat

GR50 in high concentration in stress granules likely in a gel form, promotes their conversion into pathogenic amyloid-like aggregates [78-82].

In support of this model, RNP-granule formation has been shown to be strongly associated with neurodegeneration. This was accomplished with the aid of ATXN2, an RNP-protein that is required for RNP-granule formation. Three ALS associated proteins, TDP-43, FUS and C9OFR72-encoded dipeptide repeat GR50, have been shown to co-localize with ATXN2 RNP granules [42,78] in yeast, human or Drosophila S2 cells. Also, either reducing the level of ATXN2 or deleting one of its intrinsically disordered regions both reduced RNP-granule formation and reduced neurodegeneration caused by TDP-43, C9ORF72 dipeptide or FUS [78,83-85]. These results help explain why expansions of the polyQ regions in ATXN2 that increase the stability, and thus likely the level of ATXN2, are associated with neurodegenerative disease (susceptibility to ALS and type 2 spinocerebellar ataxia).

Here, using a yeast model system we report similar effects of PBP1, the yeast ATXN2 homolog, on CREST: overexpression of PBP1 causes CREST to co-localize with PBP1 in cytoplasmic granules; deletion of *PBP1* reduces toxicity of CREST. Overexpression of PBP1 has previously been shown to induce the formation of cytoplasmic PBP1 foci [86] that recruit TORC1 thereby downregulating TORC1 function [87]. PBP1 foci may similarly attract CREST to cytoplasmic granules which may promote CREST's conversion to a more toxic form. Consistently, in a transgenic Drosophila model of CREST proteinopathy, deletion of the fly ATXN2 ortholog, dAtx2, dramatically mitigated CREST toxicity in retinal ganglion cells. Therefore, we showed that CREST is yet another protein, in addition to TDP-43, that is highly sensitive to ATXN2 dosage indicating that ATXN2 likely has a more general role as a modifier of neurotoxicity.

In mammals, endogenous CREST is a member of a chromatin remodeling complex and thereby activates transcription. When expressed in yeast, we found that CREST releases telomeric silencing and causes flocculation. Thus we propose that even in yeast the heterologous CREST protein remodels chromatin causing transcriptional activation of telomerically located genes including those that cause flocculation (e.g. *FLO1, FLO5, FLO9* and *FLO10*) as well as the epigenetically controlled gene *FLO11*. Likewise, a yeast chromatin remodeling complex protein, SWI1, is required for the

expression of telomerically located and epigenetically controlled *FLO* genes [88]. Interestingly, SWI1 can form infectious prion aggregates [12] reminiscent of the amyloid CREST aggregates seen here.

Our results extend the spectrum of ALS associated proteins that are affected by ATXN2 to include CREST. This supports the hypothesis that therapies that target ATXN2 may be effective for a wide range of neurodegenerative diseases.

Methods

Yeast strains and plasmids

Yeast strains and plasmids used are listed in Tables 1 and 2. Unless otherwise stated, yeast strain BY4741 (*MAT**a** his3Δ1 leu2Δ0 met15Δ0 ura3Δ0)* was used. Yeast transformation was by the lithium acetate method[89]. L3491 bearing an integrated copy of *ADH1-HTB1-mCh* was used to check CREST nuclear localization [37]. *FLO1* (L3580) and *FLO11 (*L3582) promoter reporter strains were respectively made from DY755 and DY758. DY755 and DY758 are Ura^+ because *FLO8,* which is disrupted in these strains, is required for regulation that inhibits the *FLO1* and *FLO11* promoters [54,90]. We obtained pop-outs of the *HIS3* disruptions of *FLO8* by selecting for Ura^- revertants on 5-FOA plates [91] and checking these for those that had become His^-. Several such pop-outs were obtained and tested and they all behaved identically. Unless otherwise stated, all overexpression plasmids were driven by the *GAL1* promoter. Gateway technology [92] was used to make CREST entry clone p*DONR-CREST* with BP reactions between pDONR221 (Invitrogen, Cat# 12536017) and a CREST fragment amplified from p*C1-CREST* with PCR. The CREST fragment in p*DONR-CREST* was further transferred to YEp*GAL-GFP*, YCp-*GAL-GFP*, YEp*GAL-DsRED* and YIp*GAL-GFP* to respectively build YEp*GAL-CREST-GFP*, YCp*GAL-CREST-GFP*, YEp*GAL-CREST-DsRED* and YIp*GAL-CREST-GFP* with LR reactions. To increase expression of *GAL1* controlled CREST, pβ-est, containing human estrogen receptor hormone-binding domain fused to the *GAL4* DNA binding domain and the VP16 viral transcriptional activator (hER) was used.

Cultivation procedures

Standard media and growth conditions were used [93,94]. All liquid-culture experiments were carried out with mid-log-phase cells. Complex (YPD) yeast media contained 2% dextrose. Synthetic medium lacked a specific component, e.g. leucine, and contained 2% dextrose, e.g., SD-Leu (-Leu medium) or 2% galactose without (SGal-Leu) or with raffinose 2% (SRGal-Leu). Cells co-transformed with pβest, containing hER, were grown in β-estradiol (1 μM) in glucose media to turn on expression of *GAL1* controlled CREST [55],[56]. FOA medium containing 12 mg/l 5-fluoro-orotic acid and 12 mg/l uracil was used to select for Ura^- cells [91]. To prevent the accumulation of suppressor mutants that reverse CREST toxicity, pGAL1-CREST transformants were maintained on plasmid selective SD medium where CREST was not expressed. Patches were then replica-plated onto synthetic glycerol (2%) to identify petites that were dropped from further study. To analyze growth, non-petite transformants from SD plates were normalized in water to an OD_{600} of 2 and serially diluted 10X. Finally about 5μl of diluted cell suspensions were spotted on plasmid selective SD, SGal or SD + β-estradiol using an MC48 (Dan-kar Corp, MA) spotter.

Western blot analysis

CREST was detected in pre-cleared lysates separated by SDS-Page and blotted as described previously [95]. For analysis of proteins in total lysate vs. supernatant and pellet, the pellet from 90 μg of total lysate centrifuged at 50K rpm for 6 min was resuspended in water to the initial volume of total lysate centrifuged. The same sample volumes of total lysate, supernatant and pellet were then separated by SDS-Page. Blots were developed with GFP mouse antibody from Roche Applied Science (Indianapolis, IN) and PGK antibody from life technologies (Frederick, MD).

Visualization of aggregates and co-localization studies

Fluorescently labeled protein aggregates, were visualized in cells with a Nikon Eclipse E600 fluorescent microscope (100X oil immersion) equipped with FITC, YFP and mCh (respectively, chroma 49011, 49003 and 49008) filter cubes. To visualize nuclei, cells with the integrated HTB1-mCh nuclear marker were used [37].

Flocculation Assay

Flocculation was assayed by resuspending a sample of each 2 d culture grown in plasmid selective SRGal in 50 mM EDTA in water. Since flocculation requires the presence of Ca^{2+} ions [96], the EDTA removed clumping so OD_{600} of cells could be accurately measured. Then another sample of cells that was not treated with EDTA was appropriately normalized to OD_{600} =10. Cells were photographed after they were allowed to settle for 15 min. The level of precipitation of cells and the reduction in the OD of the supernatants (diluted 10X) is a measure of
the flocculence.

Thioflavin T Staining

Yeast cells were stained with thioflavin T according to a protocol adapted from [31] with the addition of two extra washes in PMST [0.1M KPO4 (pH 7.5), 1 mM MgCl2, 1 M Sorbitol, 0.1% Tween 20].

Generation and characterization of transgenic flies

Generation of human CREST lines used in this study has been described earlier [52]. gmr-GAL4, UAS-lacZ and dAtx2 ^{06490} lines were obtained from the Bloomington Drosophila stock center. Fly stocks were raised on standard Drosophila medium at 20 °C. Crosses between the Drosophila strains were carried out at 25 °C using standard procedures. For histochemical analyses, heads of 5-day-old adult transgenic flies were dissected, collected, briefly washed in phosphate buffered saline (PBS), and fixed with 4% paraformaldehyde containing 0.1% Triton X-100 at room temperature for 2 hours. After a brief wash in PBS, tissues were dehydrated by graded ethanol, cleared in butanol and embedded in paraffin. Four-micrometer thick coronal sections were stained with hematoxylin and eosin (H&E).

Data Availability

No datasets were generated during the current study. The datasets analyzed during the current study are publically available at https://www.yeastgenome.org/.

REFERENCES

1. Bertram L, Tanzi RE (2005) The genetic epidemiology of neurodegenerative disease. J Clin Invest 115: 1449-1457.
2. Chen S, Sayana P, Zhang X, Le W (2013) Genetics of amyotrophic lateral sclerosis: an update. Mol Neurodegener 8: 28.
3. Barmada SJ, Skibinski G, Korb E, Rao EJ, Wu JY, et al. (2010) Cytoplasmic mislocalization of TDP-43 is toxic to neurons and enhanced by a mutation associated with familial amyotrophic lateral sclerosis. J Neurosci 30: 639-649.
4. Liebman SW, Chernoff YO (2012) Prions in yeast. Genetics 191: 1041-1072.
5. Wickner RB (1994) [URE3] as an altered URE2 protein: evidence for a prion analog in Saccharomyces cerevisiae. Science 264: 566-569.
6. Wickner RB, Masison DC, Edskes HK (1995) [PSI] and [URE3] as yeast prions. Yeast 11: 1671-1685.
7. Sondheimer N, Lindquist S (2000) Rnq1: an epigenetic modifier of protein function in yeast. Mol Cell 5: 163-172.
8. Derkatch IL, Bradley ME, Hong JY, Liebman SW (2001) Prions affect the appearance of other prions: the story of [PIN(+)]. Cell 106: 171-182.
9. Patel BK, Gavin-Smyth J, Liebman SW (2009) The yeast global transcriptional co-repressor protein Cyc8 can propagate as a prion. Nat Cell Biol 11: 344-349.
10. Suzuki G, Shimazu N, Tanaka M (2012) A yeast prion, Mod5, promotes acquired drug resistance and cell survival under environmental stress. Science 336: 355-359.
11. Patino MM, Liu JJ, Glover JR, Lindquist S (1996) Support for the prion hypothesis for inheritance of a phenotypic trait in yeast. Science 273: 622-626.
12. Du Z, Park KW, Yu H, Fan Q, Li L (2008) Newly identified prion linked to the chromatin-remodeling factor Swi1 in Saccharomyces cerevisiae. Nat Genet 40: 460-465.
13. Paushkin SV, Kushnirov VV, Smirnov VN, Ter-Avanesyan MD (1996) Propagation of the yeast prion-like [psi+] determinant is mediated by oligomerization of the SUP35-encoded polypeptide chain release factor. EMBO J 15: 3127-3134.
14. Nizhnikov AA, Alexandrov AI, Ryzhova TA, Mitkevich OV, Dergalev AA, et al. (2014) Proteomic screening for amyloid proteins. PLoS One 9: e116003.
15. Pezza JA, Villali J, Sindi SS, Serio TR (2014) Amyloid-associated activity contributes to the severity and toxicity of a prion phenotype. Nat Commun 5: 4384.
16. Du Z, Li L (2014) Investigating the interactions of yeast prions: [SWI+], [PSI+], and [PIN+]. Genetics 197: 685-700.
17. Derkatch IL, Bradley ME, Zhou P, Chernoff YO, Liebman SW (1997) Genetic and environmental factors affecting the de novo appearance of the [PSI+] prion in Saccharomyces cerevisiae. Genetics 147: 507-519.
18. Derkatch IL, Uptain SM, Outeiro TF, Krishnan R, Lindquist SL, et al. (2004) Effects of Q/N-rich, polyQ, and non-polyQ amyloids on the de novo formation of the [PSI+] prion in yeast and aggregation of Sup35 in vitro. Proc Natl Acad Sci U S A 101: 12934-12939.
19. Liebman SW, Bagriantsev SN, Derkatch IL (2006) Biochemical and genetic methods for characterization of [PIN+] prions in yeast. Methods 39: 23-34.
20. Derkatch IL, Liebman SW (2007) Prion-prion interactions. Prion 1: 161-169.
21. Sharma J, Liebman SW (2013) Exploring the basis of [PIN(+)] variant differences in [PSI(+)] induction. J Mol Biol 425: 3046-3059.
22. Sharma J, Liebman SW (2013) Variant-specific prion interactions: Complicating factors. Cell Logist 3: e25698.
23. Vitrenko YA, Gracheva EO, Richmond JE, Liebman SW (2007) Visualization of aggregation of the Rnq1 prion domain and cross-seeding interactions with Sup35NM. J Biol Chem 282: 1779-1787.
24. Yang Z, Hong JY, Derkatch IL, Liebman SW (2013) Heterologous gln/asn-rich proteins impede the propagation of yeast prions by altering chaperone availability. PLoS Genet 9: e1003236.

25. Serio TR (2018) [PIN+]ing down the mechanism of prion appearance. FEMS Yeast Res 18.
26. Osherovich LZ, Weissman JS (2001) Multiple Gln/Asn-rich prion domains confer susceptibility to induction of the yeast [PSI(+)] prion. Cell 106: 183-194.
27. Khan T, Kandola TS, Wu J, Venkatesan S, Ketter E, et al. (2018) Quantifying Nucleation In Vivo Reveals the Physical Basis of Prion-like Phase Behavior. Mol Cell 71: 155-168 e157.
28. Meriin AB, Zhang X, He X, Newnam GP, Chernoff YO, et al. (2002) Huntington toxicity in yeast model depends on polyglutamine aggregation mediated by a prion-like protein Rnq1. J Cell Biol 157: 997-1004.
29. Gokhale KC, Newnam GP, Sherman MY, Chernoff YO (2005) Modulation of prion-dependent polyglutamine aggregation and toxicity by chaperone proteins in the yeast model. J Biol Chem 280: 22809-22818.
30. Holmes DL, Lancaster AK, Lindquist S, Halfmann R (2013) Heritable remodeling of yeast multicellularity by an environmentally responsive prion. Cell 153: 153-165.
31. Johnson BS, McCaffery JM, Lindquist S, Gitler AD (2008) A yeast TDP-43 proteinopathy model: Exploring the molecular determinants of TDP-43 aggregation and cellular toxicity. Proc Natl Acad Sci U S A 105: 6439-6444.
32. Ju S, Tardiff DF, Han H, Divya K, Zhong Q, et al. (2011) A yeast model of FUS/TLS-dependent cytotoxicity. PLoS Biol 9: e1001052.
33. Kryndushkin D, Ihrke G, Piermartiri TC, Shewmaker F (2012) A yeast model of optineurin proteinopathy reveals a unique aggregation pattern associated with cellular toxicity. Mol Microbiol 86: 1531-1547.
34. Kryndushkin D, Shewmaker F (2011) Modeling ALS and FTLD proteinopathies in yeast: an efficient approach for studying protein aggregation and toxicity. Prion 5: 250-257.
35. Di Gregorio SE, Duennwald ML (2018) Yeast as a model to study protein misfolding in aged cells. FEMS Yeast Res 18.
36. Kurahashi H, Ishiwata M, Shibata S, Nakamura Y (2008) A regulatory role of the Rnq1 nonprion domain for prion propagation and polyglutamine aggregates. Mol Cell Biol 28: 3313-3323.
37. Park SK, Hong JY, Arslan F, Kanneganti V, Patel B, et al. (2017) Overexpression of the essential Sis1 chaperone reduces TDP-43 effects on toxicity and proteolysis. PLoS Genet 13: e1006805.
38. Treusch S, Hamamichi S, Goodman JL, Matlack KE, Chung CY, et al. (2011) Functional links between Abeta toxicity, endocytic trafficking, and Alzheimer's disease risk factors in yeast. Science 334: 1241-1245.
39. Park SK, Ratia K, Ba M, Valencik M, Liebman SW (2016) Inhibition of Abeta42 oligomerization in yeast by a PICALM ortholog and certain FDA approved drugs. Microb Cell 3: 53-64.
40. Rosenthal SL, Wang X, Demirci FY, Barmada MM, Ganguli M, et al. (2012) Beta-amyloid toxicity modifier genes and the risk of Alzheimer's disease. Am J Neurodegener Dis 1: 191-198.
41. Gitler AD, Chesi A, Geddie ML, Strathearn KE, Hamamichi S, et al. (2009) Alpha-synuclein is part of a diverse and highly conserved interaction network that includes PARK9 and manganese toxicity. Nat Genet 41: 308-315.
42. Elden AC, Kim HJ, Hart MP, Chen-Plotkin AS, Johnson BS, et al. (2010) Ataxin-2 intermediate-length polyglutamine expansions are associated with increased risk for ALS. Nature 466: 1069-1075.
43. Auburger G, Sen NE, Meierhofer D, Basak AN, Gitler AD (2017) Efficient Prevention of Neurodegenerative Diseases by Depletion of Starvation Response Factor Ataxin-2. Trends Neurosci 40: 507-516.
44. Figley MD, Thomas A, Gitler AD (2014) Evaluating noncoding nucleotide repeat expansions in amyotrophic lateral sclerosis. Neurobiol Aging 35: 936 e931-934.
45. Gispert S, Kurz A, Waibel S, Bauer P, Liepelt I, et al. (2012) The modulation of Amyotrophic Lateral Sclerosis risk by ataxin-2 intermediate polyglutamine expansions is a specific effect. Neurobiol Dis 45: 356-361.
46. Yu Z, Zhu Y, Chen-Plotkin AS, Clay-Falcone D, McCluskey L, et al. (2011) PolyQ repeat expansions in ATXN2 associated with ALS are CAA interrupted repeats. PLoS One 6: e17951.

47. Teyssou E, Vandenberghe N, Moigneu C, Boillee S, Couratier P, et al. (2014) Genetic analysis of SS18L1 in French amyotrophic lateral sclerosis. Neurobiol Aging 35.
48. Chesi A, Staahl BT, Jovicic A, Couthouis J, Fasolino M, et al. (2013) Exome sequencing to identify de novo mutations in sporadic ALS trios. Nat Neurosci 16: 851-855.
49. Middeljans E, Wan X, Jansen PW, Sharma V, Stunnenberg HG, et al. (2012) SS18 together with animal-specific factors defines human BAF-type SWI/SNF complexes. PLoS One 7: e33834.
50. Hodges C, Kirkland JG, Crabtree GR (2016) The Many Roles of BAF (mSWI/SNF) and PBAF Complexes in Cancer. Cold Spring Harb Perspect Med 6.
51. Staahl BT, Tang J, Wu W, Sun A, Gitler AD, et al. (2013) Kinetic analysis of npBAF to nBAF switching reveals exchange of SS18 with CREST and integration with neural developmental pathways. J Neurosci 33: 10348-10361.
52. Kukharsky MS, Quintiero A, Matsumoto T, Matsukawa K, An H, et al. (2015) Calcium-responsive transactivator (CREST) protein shares a set of structural and functional traits with other proteins associated with amyotrophic lateral sclerosis. Mol Neurodegener 10: 20.
53. Pradhan A, Liu Y (2005) A multifunctional domain of the calcium-responsive transactivator (CREST) that inhibits dendritic growth in cultured neurons. J Biol Chem 280: 24738-24743.
54. Du Z, Zhang Y, Li L (2015) The Yeast Prion [SWI(+)] Abolishes Multicellular Growth by Triggering Conformational Changes of Multiple Regulators Required for Flocculin Gene Expression. Cell Rep 13: 2865-2878.
55. Louvion JF, Havaux-Copf B, Picard D (1993) Fusion of GAL4-VP16 to a steroid-binding domain provides a tool for gratuitous induction of galactose-responsive genes in yeast. Gene 131: 129-134.
56. Derkatch IL, Chernoff YO, Kushnirov VV, Inge-Vechtomov SG, Liebman SW (1996) Genesis and variability of [PSI] prion factors in Saccharomyces cerevisiae. Genetics 144: 1375-1386.
57. Park SK, Arslan F, Kanneganti V, Barmada SJ, Purushothaman P, et al. (2018) Overexpression of a conserved HSP40 chaperone reduces toxicity of several neurodegenerative disease proteins. Prion 12: 16-22.
58. Chernoff YO, Lindquist SL, Ono B, Inge-Vechtomov SG, Liebman SW (1995) Role of the chaperone protein Hsp104 in propagation of the yeast prion-like factor [psi+]. Science 268: 880-884.
59. Halme A, Bumgarner S, Styles C, Fink GR (2004) Genetic and epigenetic regulation of the FLO gene family generates cell-surface variation in yeast. Cell 116: 405-415.
60. Fushimi K, Long C, Jayaram N, Chen X, Li L, et al. (2011) Expression of human FUS/TLS in yeast leads to protein aggregation and cytotoxicity, recapitulating key features of FUS proteinopathy. Protein Cell 2: 141-149.
61. Satterfield TF, Jackson SM, Pallanck LJ (2002) A Drosophila homolog of the polyglutamine disease gene SCA2 is a dosage-sensitive regulator of actin filament formation. Genetics 162: 1687-1702.
62. Zhou P, Derkatch IL, Liebman SW (2001) The relationship between visible intracellular aggregates that appear after overexpression of Sup35 and the yeast prion-like elements [PSI(+)] and [PIN(+)]. Mol Microbiol 39: 37-46.
63. Derkatch IL, Bradley ME, Masse SV, Zadorsky SP, Polozkov GV, et al. (2000) Dependence and independence of [PSI(+)] and [PIN(+)]: a two-prion system in yeast? EMBO J 19: 1942-1952.
64. Fuentealba RA, Udan M, Bell S, Wegorzewska I, Shao J, et al. (2010) Interaction with polyglutamine aggregates reveals a Q/N-rich domain in TDP-43. J Biol Chem 285: 26304-26314.
65. Doi H, Okamura K, Bauer PO, Furukawa Y, Shimizu H, et al. (2008) RNA-binding protein TLS is a major nuclear aggregate-interacting protein in huntingtin exon 1 with expanded polyglutamine-expressing cells. J Biol Chem 283: 6489-6500.
66. Seidel G, Meierhofer D, Sen NE, Guenther A, Krobitsch S, et al. (2017) Quantitative Global Proteomics of Yeast PBP1 Deletion Mutants and Their Stress Responses Identifies Glucose Metabolism, Mitochondrial, and Stress Granule Changes. J Proteome Res 16: 504-515.
67. Olbertz JH (2012) The protein SS18L1 is a potent suppressor of polyQ mediated huntingtin aggregation and toxicity. Dissertation Adviser Dr. Erich Wanker.

68. Kapeli K, Pratt GA, Vu AQ, Hutt KR, Martinez FJ, et al. (2016) Distinct and shared functions of ALS-associated proteins TDP-43, FUS and TAF15 revealed by multisystem analyses. Nat Commun 7: 12143.
69. Couthouis J, Hart MP, Shorter J, DeJesus-Hernandez M, Erion R, et al. (2011) A yeast functional screen predicts new candidate ALS disease genes. Proc Natl Acad Sci U S A 108: 20881-20890.
70. Neumann M, Sampathu DM, Kwong LK, Truax AC, Micsenyi MC, et al. (2006) Ubiquitinated TDP-43 in frontotemporal lobar degeneration and amyotrophic lateral sclerosis. Science 314: 130-133.
71. Kwiatkowski TJ, Jr., Bosco DA, Leclerc AL, Tamrazian E, Vanderburg CR, et al. (2009) Mutations in the FUS/TLS gene on chromosome 16 cause familial amyotrophic lateral sclerosis. Science 323: 1205-1208.
72. Vance C, Rogelj B, Hortobagyi T, De Vos KJ, Nishimura AL, et al. (2009) Mutations in FUS, an RNA processing protein, cause familial amyotrophic lateral sclerosis type 6. Science 323: 1208-1211.
73. Jovicic A, Paul JW, 3rd, Gitler AD (2016) Nuclear transport dysfunction: a common theme in amyotrophic lateral sclerosis and frontotemporal dementia. J Neurochem 138 Suppl 1: 134-144.
74. Archbold HC, Jackson KL, Arora A, Weskamp K, Tank EM, et al. (2018) TDP43 nuclear export and neurodegeneration in models of amyotrophic lateral sclerosis and frontotemporal dementia. Sci Rep 8: 4606.
75. Kryndushkin D, Wickner RB, Shewmaker F (2011) FUS/TLS forms cytoplasmic aggregates, inhibits cell growth and interacts with TDP-43 in a yeast model of amyotrophic lateral sclerosis. Protein Cell 2: 223-236.
76. Armakola M, Higgins MJ, Figley MD, Barmada SJ, Scarborough EA, et al. (2012) Inhibition of RNA lariat debranching enzyme suppresses TDP-43 toxicity in ALS disease models. Nat Genet 44: 1302-1309.
77. Sun Z, Diaz Z, Fang X, Hart MP, Chesi A, et al. (2011) Molecular determinants and genetic modifiers of aggregation and toxicity for the ALS disease protein FUS/TLS. PLoS Biol 9: e1000614.
78. Bakthavachalu B, Huelsmeier J, Sudhakaran IP, Hillebrand J, Singh A, et al. (2018) RNP-Granule Assembly via Ataxin-2 Disordered Domains Is Required for Long-Term Memory and Neurodegeneration. Neuron 98: 754-766 e754.
79. Li YR, King OD, Shorter J, Gitler AD (2013) Stress granules as crucibles of ALS pathogenesis. J Cell Biol 201: 361-372.
80. Maharana S, Wang J, Papadopoulos DK, Richter D, Pozniakovsky A, et al. (2018) RNA buffers the phase separation behavior of prion-like RNA binding proteins. Science 360: 918-921.
81. Li S, Zhang P, Freibaum BD, Kim NC, Kolaitis RM, et al. (2016) Genetic interaction of hnRNPA2B1 and DNAJB6 in a Drosophila model of multisystem proteinopathy. Hum Mol Genet 25: 936-950.
82. Monahan Z, Shewmaker F, Pandey UB (2016) Stress granules at the intersection of autophagy and ALS. Brain Res 1649: 189-200.
83. Becker LA, Huang B, Bieri G, Ma R, Knowles DA, et al. (2017) Therapeutic reduction of ataxin-2 extends lifespan and reduces pathology in TDP-43 mice. Nature 544: 367-371.
84. Lee KH, Zhang P, Kim HJ, Mitrea DM, Sarkar M, et al. (2016) C9orf72 Dipeptide Repeats Impair the Assembly, Dynamics, and Function of Membrane-Less Organelles. Cell 167: 774-788 e717.
85. Scoles DR, Meera P, Schneider MD, Paul S, Dansithong W, et al. (2017) Antisense oligonucleotide therapy for spinocerebellar ataxia type 2. Nature 544: 362-366.
86. Swisher KD, Parker R (2010) Localization to, and effects of Pbp1, Pbp4, Lsm12, Dhh1, and Pab1 on stress granules in Saccharomyces cerevisiae. PLoS One 5: e10006.
87. Takahara T, Maeda T (2012) Transient sequestration of TORC1 into stress granules during heat stress. Mol Cell 47: 242-252.
88. Goncharoff DK, Du Z, Li L (2018) A brief overview of the Swi1 prion-[SWI+]. FEMS Yeast Res 18.
89. Gietz RD, Schiestl RH (2007) High-efficiency yeast transformation using the LiAc/SS carrier DNA/PEG method. Nat Protoc 2: 31-34.

90. Kobayashi O, Yoshimoto H, Sone H (1999) Analysis of the genes activated by the FLO8 gene in Saccharomyces cerevisiae. Curr Genet 36: 256-261.
91. Boeke JD, LaCroute F, Fink GR (1984) A positive selection for mutants lacking orotidine-5'-phosphate decarboxylase activity in yeast: 5-fluoro-orotic acid resistance. Mol Gen Genet 197: 345-346.
92. Alberti S, Gitler AD, Lindquist S (2007) A suite of Gateway cloning vectors for high-throughput genetic analysis in Saccharomyces cerevisiae. Yeast 24: 913-919.
93. Sherman F FG, Hicks JB (1986) Methods in Yeast Genetics; Sherman F FG, Hicks JB, editor. Plainview, New York: Cold Spring Harbor Press.
94. Sikorski RS, Hieter P (1989) A system of shuttle vectors and yeast host strains designed for efficient manipulation of DNA in Saccharomyces cerevisiae. Genetics 122: 19-27.
95. Bagriantsev SN, Gracheva EO, Richmond JE, Liebman SW (2008) Variant-specific [PSI+] infection is transmitted by Sup35 polymers within [PSI+] aggregates with heterogeneous protein composition. Mol Biol Cell 19: 2433-2443.
96. Stratford M (1989) Yeast flocculation:Calcium specificity. Yeast 5: 487-496.
97. Brachmann CB, Davies A, Cost GJ, Caputo E, Li J, et al. (1998) Designer deletion strains derived from Saccharomyces cerevisiae S288C: a useful set of strains and plasmids for PCR-mediated gene disruption and other applications. Yeast 14: 115-132.
98. Winzeler EA, Shoemaker DD, Astromoff A, Liang H, Anderson K, et al. (1999) Functional characterization of the S. cerevisiae genome by gene deletion and parallel analysis. Science 285: 901-906.
99. Buchan JR, Muhlrad D, Parker R (2008) P bodies promote stress granule assembly in Saccharomyces cerevisiae. J Cell Biol 183: 441-455.
100. Hilliker A, Gao Z, Jankowsky E, Parker R (2011) The DEAD-box protein Ded1 modulates translation by the formation and resolution of an eIF4F-mRNA complex. Mol Cell 43: 962-972.
101. Aron R, Higurashi T, Sahi C, Craig EA (2007) J-protein co-chaperone Sis1 required for generation of [RNQ+] seeds necessary for prion propagation. EMBO J 26: 3794-3803.

Acknowledgements

We thank Ross Buchan, U. of Arizona; Bernd Bukau, U. Heidelberg; the late Susan Lindquist, MIT and Aaron Gitler, Stanford U., for plasmids and Zhiqiang Du and Liming Li, Northwestern U., for strains. In addition we thank William Eom for helpful comments on the manuscript. This work was supported National Institutes of Health Grant R01GM056350 (SWL). TAS is a Motor Neurone Disease Association Senior Non-Clinical fellow.

Competing Interests

The authors declare no competing interests.

TABLE 1. YEAST STRAINS USED.

Strains	Description	Reference
74D-694	*MAT***a** *ade1-14 ura3-52 leu2-3,112 trp1-289 his3-200*	[56]
L2910	74D-694 [*psi*$^-$] [*pin*$^-$]	[56]
L1749	74D-694 [*psi*$^-$] [*PIN*$^+$]	[56]
L3536	L1749 *GAL-CREST-EGFP:: LEU2*	This study
L3491	74D-694 [*psi*$^-$] [*PIN*$^+$] *HTB1-mCh*::*LEU2*	[37]
L3496	[*pin*$^-$] version of L3491	[37]
BY4741	*MAT***a** *his3Δ1 leu2Δ0 met15Δ0 ura3Δ0*	[97]
L3270	BY4741 [*psi*$^-$] [*PIN*$^+$]	[56]
L3269	BY4741 [*psi*$^-$] [*pin*$^-$]	[56]
L3539	BY4741 [*psi*$^-$] [*PIN*$^+$] *pbp1Δ::KanMX4*	[98]
L3570	BY4741 [*psi*$^-$] [*pin*$^-$] *pbp1Δ::KanMX4*	This study
L3540	BY4741 [*psi*$^-$] [*pin*$^-$] *hsp104Δ::KanMX4*	[98]
DY755	BY4741 *flo8::FLO8::HIS3 flo1Δ::FLO1*^{promoter}*-URA3*	[54]
L3580	BY4741 *flo1Δ::FLO1*^{promoter}*-URA3*	This study
DY758	BY4741 *flo8::FLO8::HIS3 flo11Δ::FLO11*^{promoter}*-URA3*	[54]
L3582	BY4741 *flo11Δ::FLO11*^{promoter}*-URA3*	This study

TABLE 2. PLASMIDS USED.

Short name and SWL Laboratory Plasmid #	**Original Plasmid Name/Description**	**Reference**
pβ-est, p798	pHCA/*GAL4(1–93).ER.VP16* (*HIS3*)	[55]
YCp*SUP35NM-GFP*, p1181	pRS413-*CUP1-SUP35NM-GFP* (*HIS3*)	[62]
YCp-*GAL-GFP*, p1764	pAG416-*GAL1-ccdB-EGFP* (*CEN*, *URA3*)	Addgene plasmid #14195
YCp*GAL-TDP-43-YFP*, p2042	pRS416-Gal-TDP-43-YFP (*CEN, URA3*)	Addgene plasmid #27447
YCp*GAL-FUS-YFP*, p2043	pAG416-*GAL1-FUS-YFP* (*CEN, URA3*)	This study
YCp*GAL-ccdB*, p2186	pAG413-*GAL-ccdB (CEN, HIS3)*	Addgene plasmid #14153
YCp*GAL-PBP1*, p2228	pBY011-*GAL1-PBP1* (*CEN, URA3*)	[42]
YCp*GAL*, p2229	pBY011-*GAL1* (*CEN, URA3*)	[92]
p*C1-CREST*, p2342	p*EGFP-C1-CREST*	[52]
p*DONR-CREST* p2370	pDONR-*CREST* without stop codon	This study
YCp*GAL-CREST-GFP, p2375*	pAG416-*GAL1-CREST-EGFP* (*CEN, URA3*)	This study
YEp*GAL-GFP,* p*2380*	pAG425-*GAL-ccdB-GFP* (2μ, *LEU2*)	Addgene plasmid #14201
YEp*GAL-CREST-GFP*, p2381	pAG425-*GAL1-CREST-EGFP* (2μ, *LEU2*)	This study
YEp*GAL-DsRED*, p2387	pAG425-*GAL-ccdB-DsRED* (2μ, *LEU2*)	Addgene plasmid #14369
YEp*GAL-CREST-DsRED*, p2389	pAG425-*GAL1-CREST-DsRED* (2μ, *LEU2*)	This study
YIp*GAL-CREST-GFP, p2391*	pAG305-*GAL1-CREST-EGFP* (*YIp*, *LEU2*)	This study
YIp*GAL-GFP*, p2425	YCpAG305-*GAL-ccdB-EGFP* (*YIp*, *LEU2*)	Addgene plasmid #14185
YCp*GAL-PBP1-EGFP*, p2444	pAG416-*GAL-PBP1-EGFP* (*CEN, URA3*)	This study
YCp*EDC3-mCh*, p2452	pRP1574, p*EDC3-mCh* (*CEN, URA3*)	[99]
YCp*DED1-mCh*, p2453	pRP2132, p*DED1-mCh* (*CEN, URA3*)	[100]
YEp*GAL-CREST-YFP*, p2471	pAG423-*GAL1-CREST-YFP* (2μ, *HIS3*)	This study
YCpRNQ-GFP, p1730	p413RNQpRnq1msGFP (*CEN, HIS3*)	[101]

Figure Legends:

Figure 1. Expression of human CREST in yeast is toxic. Shown is the growth of cells carrying vectors encoding *GAL-CREST-GFP* and a fusion protein that promotes induction of the *GAL* promoter in the presence of estradiol (pβ-est) spotted on plasmid selective glucose plates without estradiol where CREST-GFP expression is *Non-induced*, or with 1 μM β-estradiol where CREST-GFP expression *is β-Estradiol Induced*. Duplicates are independent transformants or integrants. Cells grown on plasmid selective glucose plates were diluted to OD_{600} =2 and then serially diluted 10-fold and spotted on the plates shown. The pβ-est plasmid expresses the fusion activator that is responsive to β-estradiol, and YCp*GAL-ccdB* ($pGAL^c$) was used as its control. (**a**) *CREST-GFP expressed from a CEN plasmid inhibits growth.* YCp*GAL-CREST-GFP* ($pCREST^C$) and control YCp-*GAL-GFP* ($pGFP^c$) vectors were used. (**b**) *CREST-GFP expressed from a 2μ plasmid inhibits growth.* YEp*GAL-CREST-GFP* ($pCREST^E$) and the control YEp*GAL-GFP* ($pGFP^E$) vectors were used. (**c**) *Integrated CREST-GFP is toxic.* Strain with integrated YIp*GAL-CREST-GFP* ($pCREST^I$) and parent strain lacking the integrated plasmid but containing control YEp*GAL-GFP* (*LEU2*) was used. Strain 74D-694 [PIN^+] was used for the *CEN* and integrated vector experiments (**a** and **c**) while strain BY4741 [PIN^+] was used for the 2μ vector experiments (**b**).

Figure 2. Toxicity of CREST is reduced by the absence of the [PIN^+] prion, but is not further reduced by the absence of HSP104. (**a**)*The [PIN^+] prion enhances toxicity of CREST in yeast.* Shown is the growth (as in Fig. 1) of [PIN^+] and [pin^-] BY4741 cells carrying YEp*GAL-CREST-GFP* ($pCREST^E$) or control YEp*GAL-GFP* ($pGFP^E$) and the pβ-est plasmid or empty control YCp*GAL-ccdB* ($pGAL^C$) on plasmid selective glucose media in the presence (β-Estradiol Induced) and absence (Non-induced) of β-estradiol . (**b**) *[PIN^+] and CREST aggregates do not co-localize.* [PIN^+] BY4741 carrying YEp*GAL-CREST-DsRed* (CREST-DsRed) and YCp*RNQ-GFP* (RNQ1-GFP) were grown overnight in plasmid selective galactose medium and examined with a fluorescence microscope. (**c**) *CREST still aggregates in the absence of HSP104. HSP104* (Wild-type) or *hsp104Δ* versions of [pin^-] BY4741 carrying

YEp*GAL-CREST-GFP* were grown overnight in plasmid selective galactose medium and examined with a fluorescence microscope. (**d**) *CREST remains toxic in the absence of HSP104. HSP104* (Wild-type) or *hsp104Δ* versions of [*pin*$^-$] BY4741 carrying YEp*GAL-CREST-GFP* (pCREST^E) or control YEp*GAL-GFP* (pGFP^E) vectors were serially diluted and spotted on plasmid selective glucose (Non-induced) or galactose medium (Galactose Induced).

Figure 3. Expression of CREST enhances yeast flocculation. (**a**) *CREST but not TDP-43 or FUS over expression enhances flocculation.* Shown are transformants of BY4741 [*PIN*$^+$] with: YCp*GAL-CREST-GFP* (CREST), YCp*GAL-TDP-43-YFP* (TDP-43), YCp*GAL-FUS-YFP* (FUS) or control YCp-*GAL-GFP* with the average and standard error of OD_{600} of 10X diluted supernatants after cells of 3 independent transformants were allowed to settle for 15 min. (**b**) *Expression of CREST activates the FLO1 and FLO11 promoters.* Strains deleted for *URA3* and containing either the *FLO1*(L3580) or *FLO11(*L3582) open reading frames (ORFs) replaced with the *URA3* ORF reporter, respectively *prFLO1:URA and prFLO11:URA* were transformed with YEp*GAL-CREST-GFP*(pCREST^E) or control YEp*GAL-GFP*(pGFP^E). Three independent transformants of each were spotted on plasmid selective glucose media (Non-induced), with (+Ura) or without (-Ura) uracil or plasmid selective -Ura galactose media (Gal Induced).

Figure 4. Human CREST expressed in yeast forms largely nuclear dots with occasional cytoplasmic foci. (**a**) *CREST-GFP expressed in yeast*. BY4741 [*PIN*$^+$] transformed with YEp*GAL-CREST-GFP* was induced for 6 or 24 h by growth in plasmid selective SRGal medium and examined under a fluorescent microscope. Shown is bright field plus fluorescence (left) and just fluorescence of the same field where small cytoplasmic foci can be seen better (right). (**b**) *Co-localization of wild-type CREST-GFP aggregates and nuclear marker HTB1-mCh*. [*PIN*$^+$] strain L3491 with integrated plasmid encoding ADH1-HTB1-mCh transformed with YCp*GAL-CREST-GFP* was grown on plasmid selective SRGal medium for 24 h and examined. (**c**) *CREST aggregates stain with the amyloid dye thioflavin T (ThT).* L3491 containing the HTB1-mCherry nuclear marker transformed with YEp*GAL-CREST-YFP*

(CREST-YFP), YCp*GAL-TDP-43-YFP* (TDP-43-YFP*)* as negative control, or YCp*GAL-FUS-YFP* (FUS-YFP) as a positive control, were grown in plasmid selective SRGAL medium overnight. ThT fluorescence was detected with a CFP filter. CFP was recolored green and YFP recolored red to facilitate visualization of merged pictures. Cell boundaries are drawn. (**d)** *CREST-GFP pellets equally in WT or pbp1Δ strains.* Transformants of (*WT*) and (*pbp1Δ*) with YEp*GAL-CREST-GFP* (pCREST^{E}) or control YEp*GAL-CREST-GFP (*pGFP^{E}) were grown on plasmid selective SRGal medium overnight and harvested. Total lysates were separated into *Supernatant* and *Pellet* by centrifugation. Samples were run on SDS-PAGE. The gel was immunoblotted with anti-GFP, stripped and reprobed with anti-PGK for loading control.

Figure 5. Heat stress causes relocalization of some CREST aggregates from the nucleus to the cytoplasm. CREST partially co-localizes with the DED1 stress granule and EDC3 P-body markers during heat-stress and returns to the nucleus following heat-stress. YCp*DED1-mCh* and YCp*EDC3-mCh* transformants of [*PIN*$^{+}$] 74D-694 with integrated *GAL-CREST-EGFP* were grown in plasmid selective SRaf(2%) to OD_{600}=0.3 when CREST-EGFP was induced by addition of 2% galactose for 5 h. Cells were then stressed for 20 min at 46°C. CREST-EGFP, DED-mCh and EDC3-mCh were examined before (30°C), during (46°C) and 3 h following (30°C) heat stress.

Figure 6. Effects of *PBP1* on CREST. (**a**) *Overexpression of PBP1 enhances CREST cytoplasmic aggregation*. Nine co-transformants of [*PIN*$^{+}$] or [*pin*$^{-}$] BY4741 with YEp*GAL-CREST-GFP* and either YCp*GAL-PBP1* (↑PBP1) or YCp*GAL* (Control) were patched and grown on plasmid selective glucose media, velveteen replica-plated and grown on selective SGal and examined with a fluorescent microscope. All transformants with ↑PBP1 had a dramatic increase in cytoplasmic foci compared with controls. Shown are representative cells of each type with cell membranes outlined. (**b**) *PBP1 expression does not significantly change CREST levels.* Left: Western blot of [*PIN*$^{+}$] transformed with YEp*GAL-CREST-GFP* and either YCp*GAL-PBP1* (↑PBP1) or control vector YCp*GAL*, grown in liquid

plasmid selective SRGal media for 36 h. Right: Blot of isogenic strains with (*pbp1Δ*) vs. wild-type *PBP1* (Control), expressing YEp*GAL-CREST-GFP.* Also shown (-CREST) is control YEp*GAL-GFP* instead of YEp*GAL-CREST-GFP* in *pbp1Δ* strain. Blots probed with GFP antibody to detect CREST were stripped and reprobed with phosoglycerate kinase (PGK) antibody to detect the PGK loading control. (**c**) *CREST co-localizes with PBP1 in RNP granules induced by PBP1 overexpression.* YEp*GAL-CREST-DsRED* (CREST) and YCp*GAL-PBP1-GFP* (PBP1) were co-transformed into BY4741[*PIN*$^{+}$] . Transformants patched on plasmid selective glucose medium were velveteen replica-plated, grown on selective SGal and examined with a fluorescent microscope. (**d**) *Overexpression of PBP1 is toxic.* Serial dilutions of [*PIN*$^{+}$] carrying YEp*GAL-CREST*-GFP(pCREST^{E}) or control YEp*GAL-GFP*(pGFP^{E}) and YCp*GAL-PBP1-GFP*(pPBP1) or control YCp*GAL*(pGAL^{C}) , were spotted on plasmid selective dextrose (Non-inducing) and galactose (Gal inducing) plates, and photographed after 3 (dextrose) or 4 (galactose) days at 30˚C**.** (**e**) *Deletion of PBP1 reduces CREST toxicity.* Independent transformants of [*PIN*$^{+}$] or [*pin*$^{-}$] without (*WT*) and with the deletion (***pbp1Δ***) carrying YEp*GAL-CREST-GFP* (pCREST^{E}) or empty GFP control YEp*GAL-GFP*(pGFP^{E}) and all carrying pβ-est expressing the fusion activator responsive to β-estradiol, were spotted and grown on plasmid selective media with (β-est Induced), and without (Non-induced), β-estradiol.

Figure 7. Heterozygous deletion of the Drosophila ortholog of ATXN2, dAtaxin2, reduced retinal degeneration induced by human CREST. H&E staining of retinal sections of 5-day-old flies reveals severe disruption of regularly ordered arrays of photoreceptor neurons in human CRESTwt TG flies, but this phenotype is completely rescued upon heterozygous deletion of dAtx2 (CRESTwt TG x dAtx2$^{06490/+}$ line). Representative images for each transgenic fly line are shown. Scale bar is 100 um.

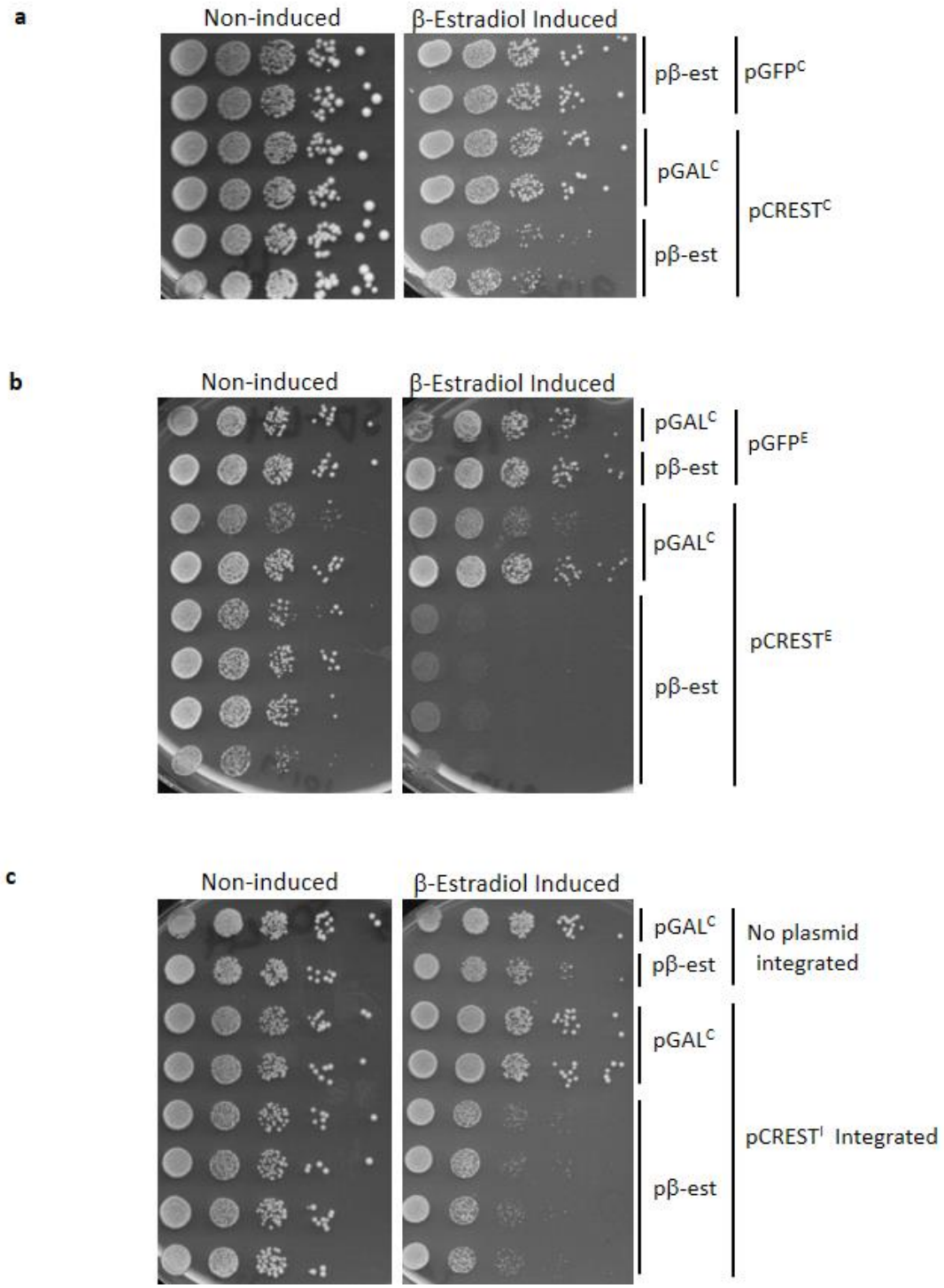
a
Non-induced
β-Estradiol Induced
pβ-est
pGFP^C
pGAL^C
pCREST^C
pβ-est
b
Non-induced
β-Estradiol Induced
pGAL^C
pβ-est
pGFP^E
pGAL^C
pCREST^E
pβ-est
c
Non-induced
β-Estradiol Induced
pGAL^C
pβ-est
No plasmid integrated
pGAL^C
pCREST^I Integrated
pβ-est

Fig. 1

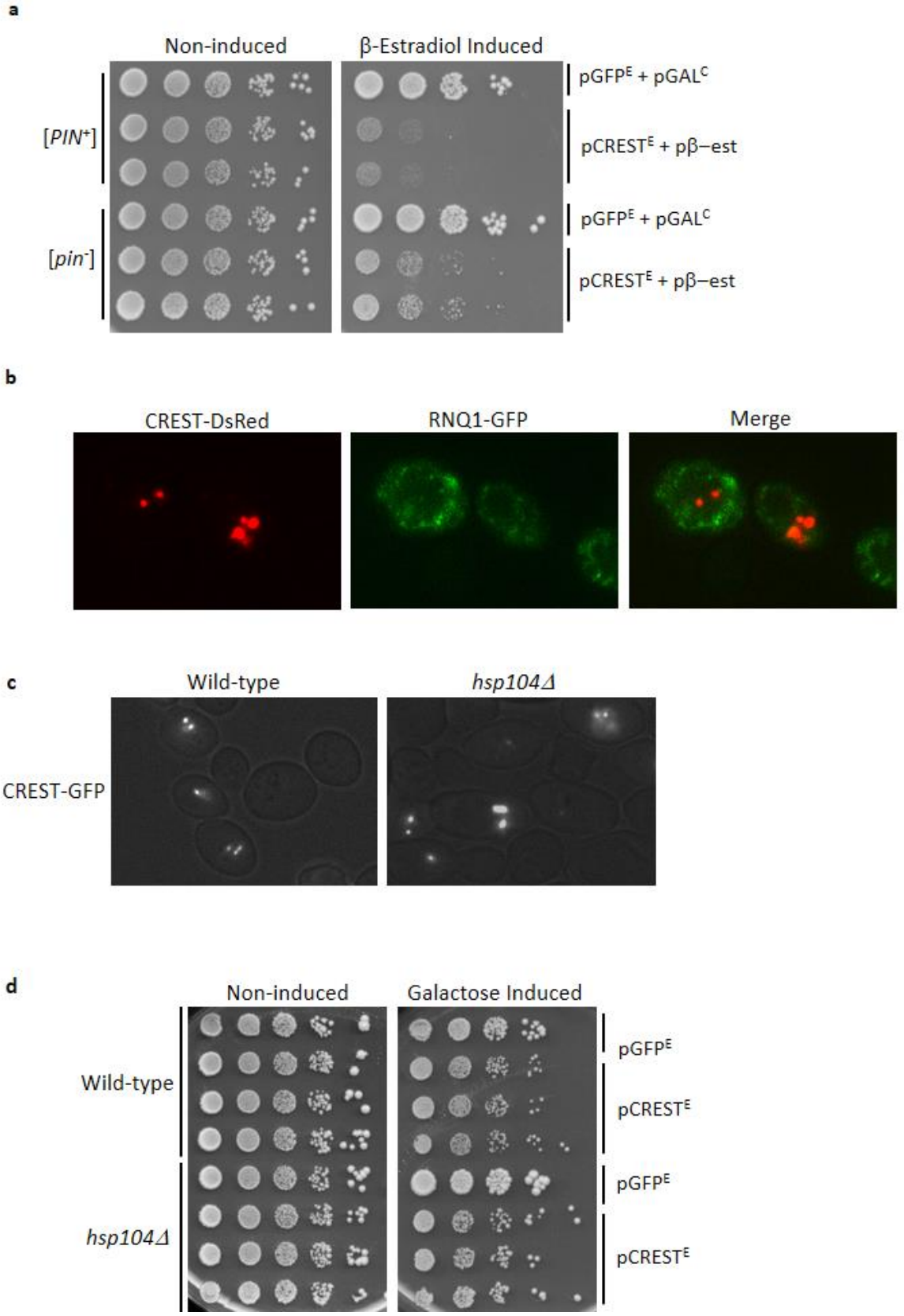
a
Non-induced
β-Estradiol Induced
[PIN+]
[pin-]
pGFPE + pGALC
pCRESTE + pβ–est
pGFPE + pGALC
pCRESTE + pβ–est
b
CREST-DsRed
RNQ1-GFP
Merge
c
Wild-type
hsp104Δ
CREST-GFP
d
Non-induced
Galactose Induced
Wild-type
hsp104Δ
pGFPE
pCRESTE
pGFPE
pCRESTE

Fig. 2

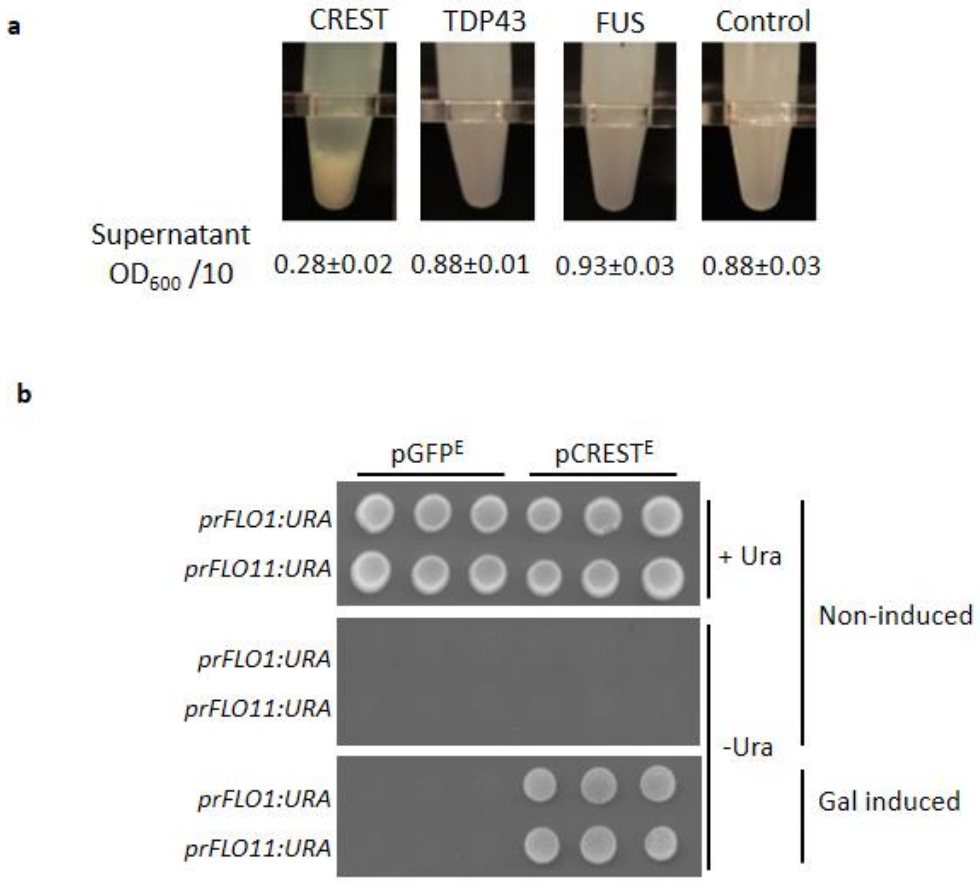
a
CREST
TDP43
FUS
Control
Supernatant
OD600 /10
0.28±0.02
0.88±0.01
0.93±0.03
0.88±0.03
b
pGFPE
pCRESTE
prFLO1:URA
prFLO11:URA
+ Ura
Non-induced
prFLO1:URA
prFLO11:URA
-Ura
prFLO1:URA
prFLO11:URA
Gal induced

Fig. 3

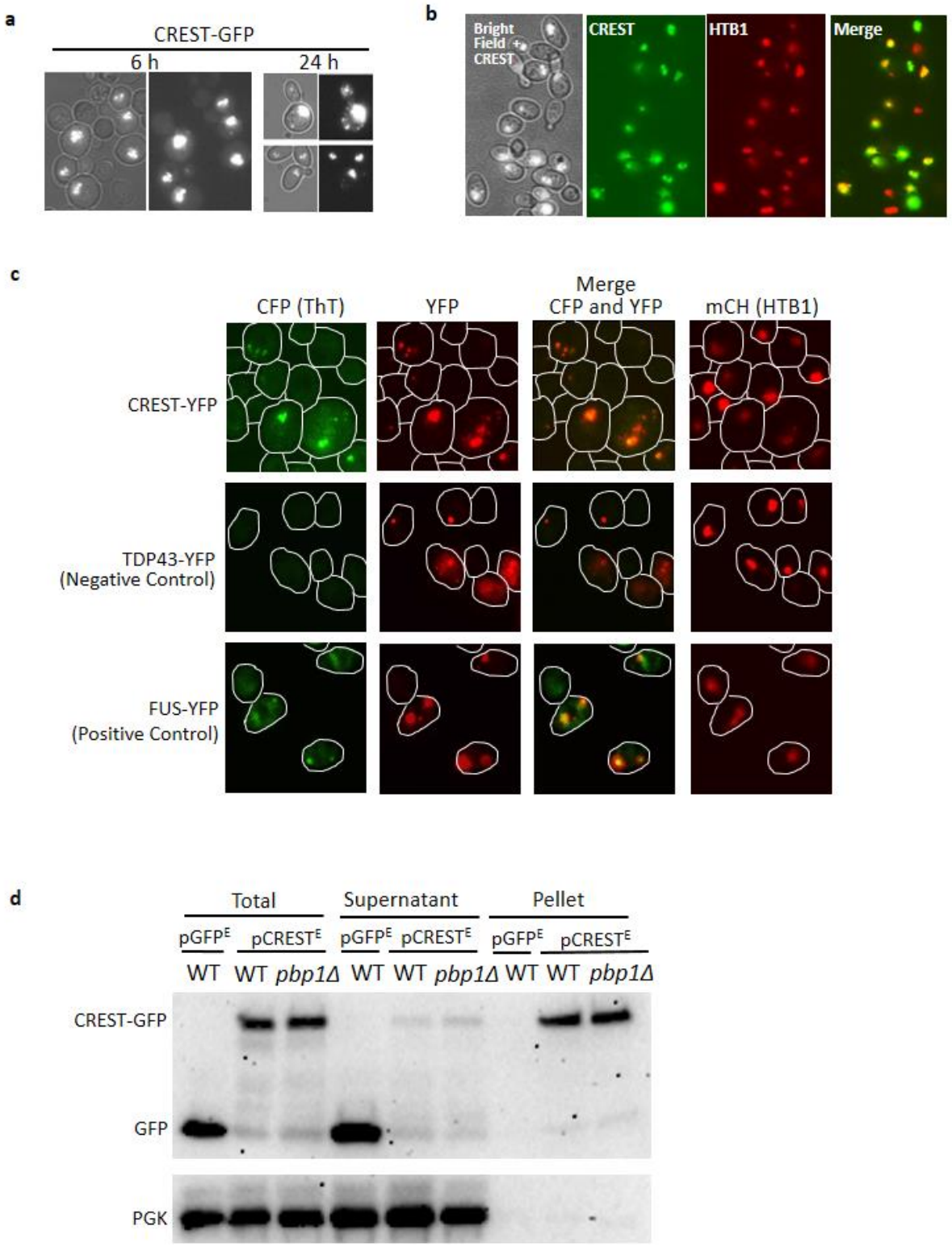
a
CREST-GFP
6 h
24 h
b
Bright Field + CREST
CREST
HTB1
Merge
c
CFP (ThT)
YFP
Merge CFP and YFP
mCH (HTB1)
CREST-YFP
TDP43-YFP (Negative Control)
FUS-YFP (Positive Control)
d
Total
Supernatant
Pellet
pGFP^E
pCREST^E
WT
WT
pbp1Δ
CREST-GFP
GFP
PGK

Fig. 4

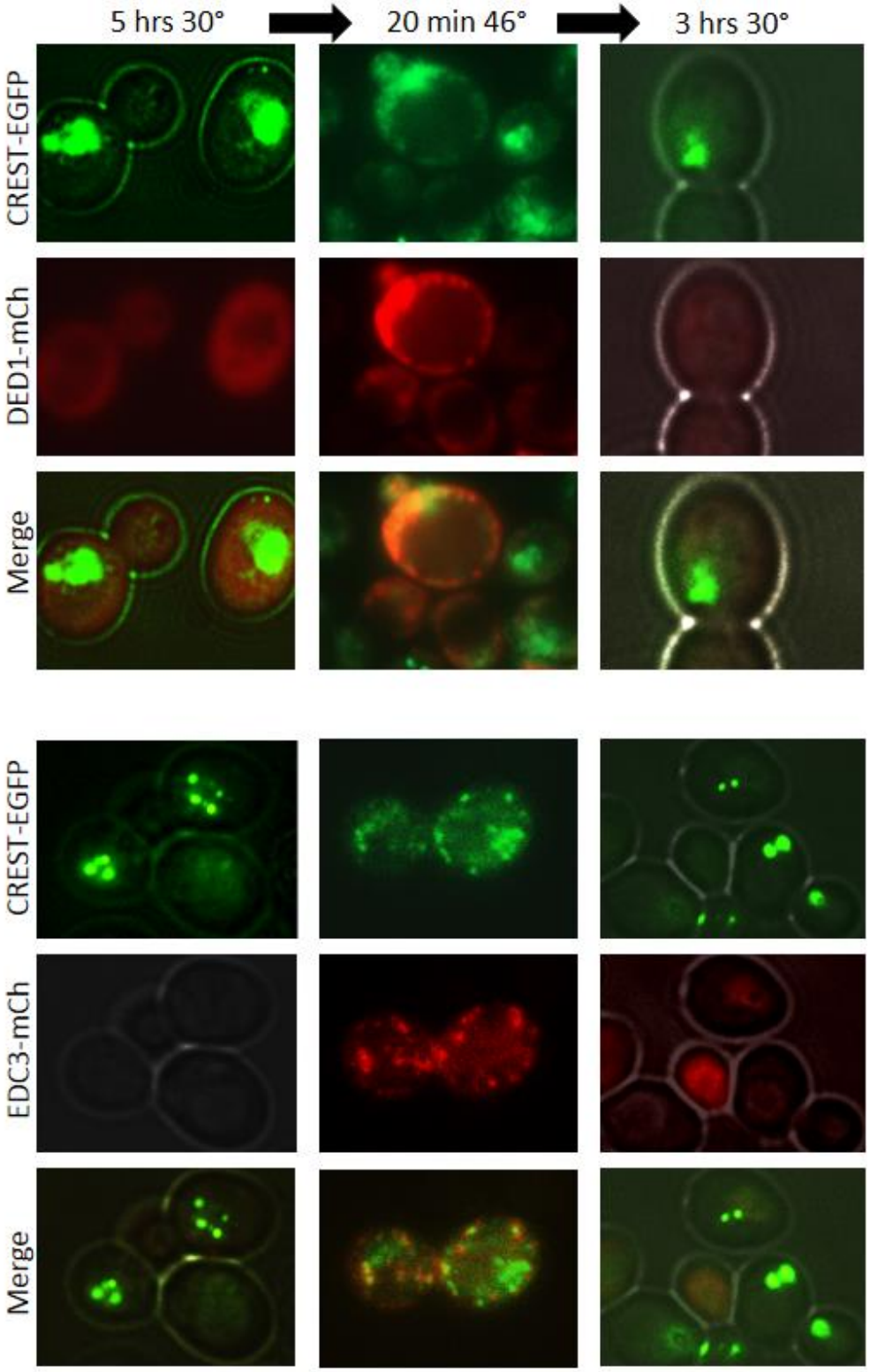
5 hrs 30°
20 min 46°
3 hrs 30°
CREST-EGFP
DED1-mCh
Merge
CREST-EGFP
EDC3-mCh
Merge

Fig. 5

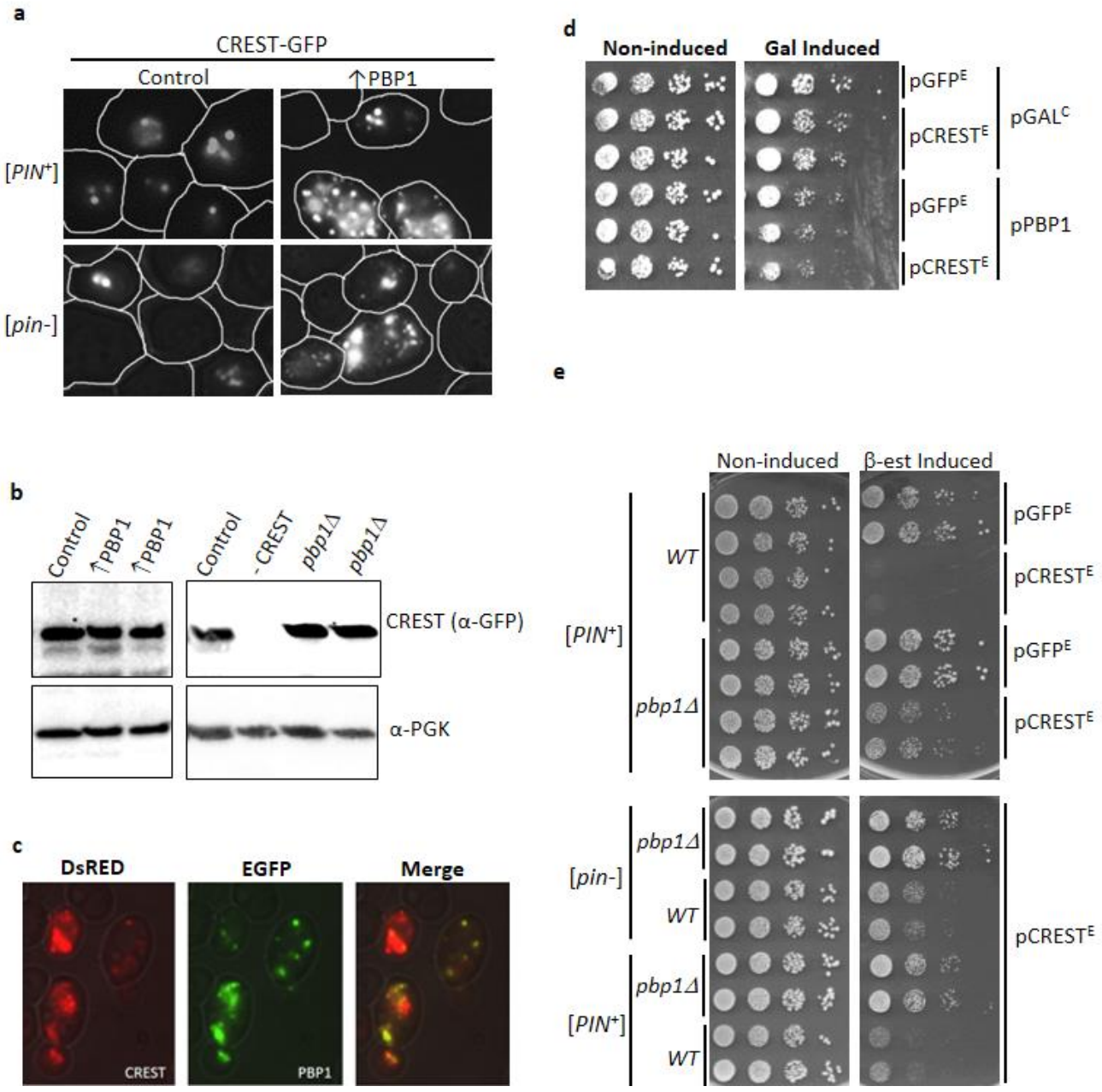
a
CREST-GFP
Control
↑PBP1
[PIN+]
[pin-]
b
Control
↑PBP1
↑PBP1
Control
- CREST
pbp1Δ
pbp1Δ
CREST (α-GFP)
α-PGK
c
DsRED
EGFP
Merge
CREST
PBP1
d
Non-induced
Gal Induced
pGFPE
pCRESTE
pGALC
pGFPE
pCRESTE
pPBP1
e
Non-induced
β-est Induced
[PIN+]
WT
pbp1Δ
pGFPE
pCRESTE
pGFPE
pCRESTE
[pin-]
pbp1Δ
WT
[PIN+]
pbp1Δ
WT
pCRESTE

Fig. 6

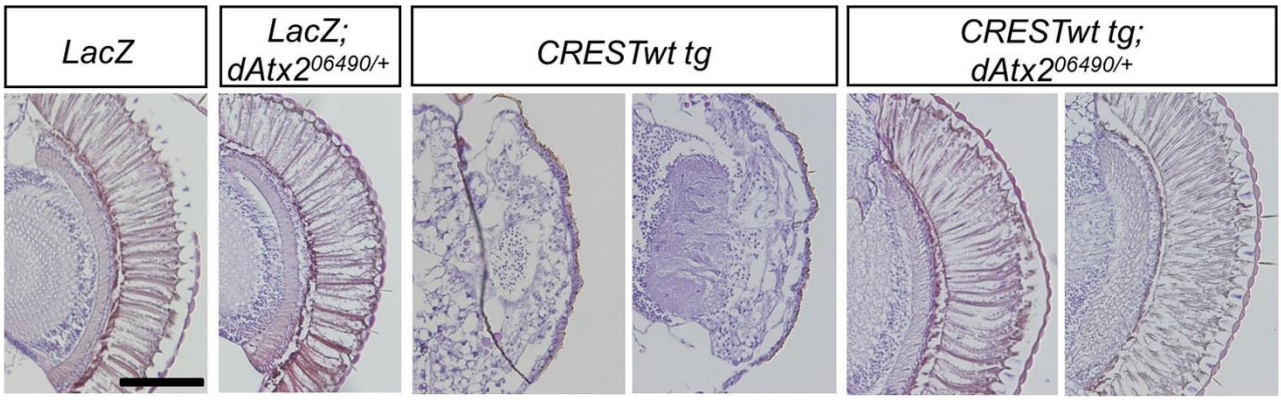

Fig. 7

Supporting information

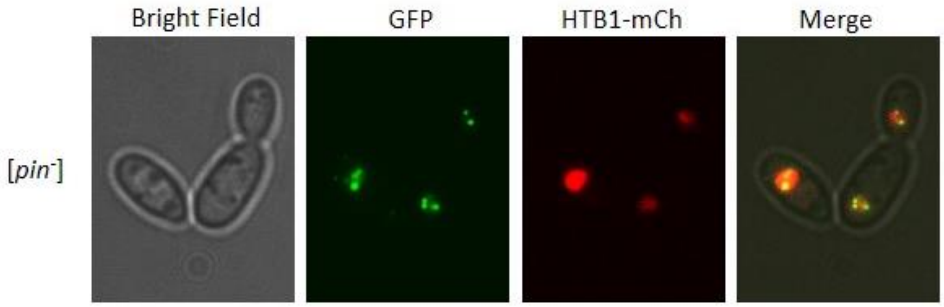

Figure S1. Co-localization of wild-type CREST-GFP aggregates and nuclear marker HTB1-mCh in [*pin*$^-$] strain. The [*pin*$^-$] strain L3496 with integrated plasmid encoding ADH1-HTB1-mCh transformed with YCp*GAL-CREST-GFP* was grown on plasmid selective SRGal medium for 24 hs and examined.

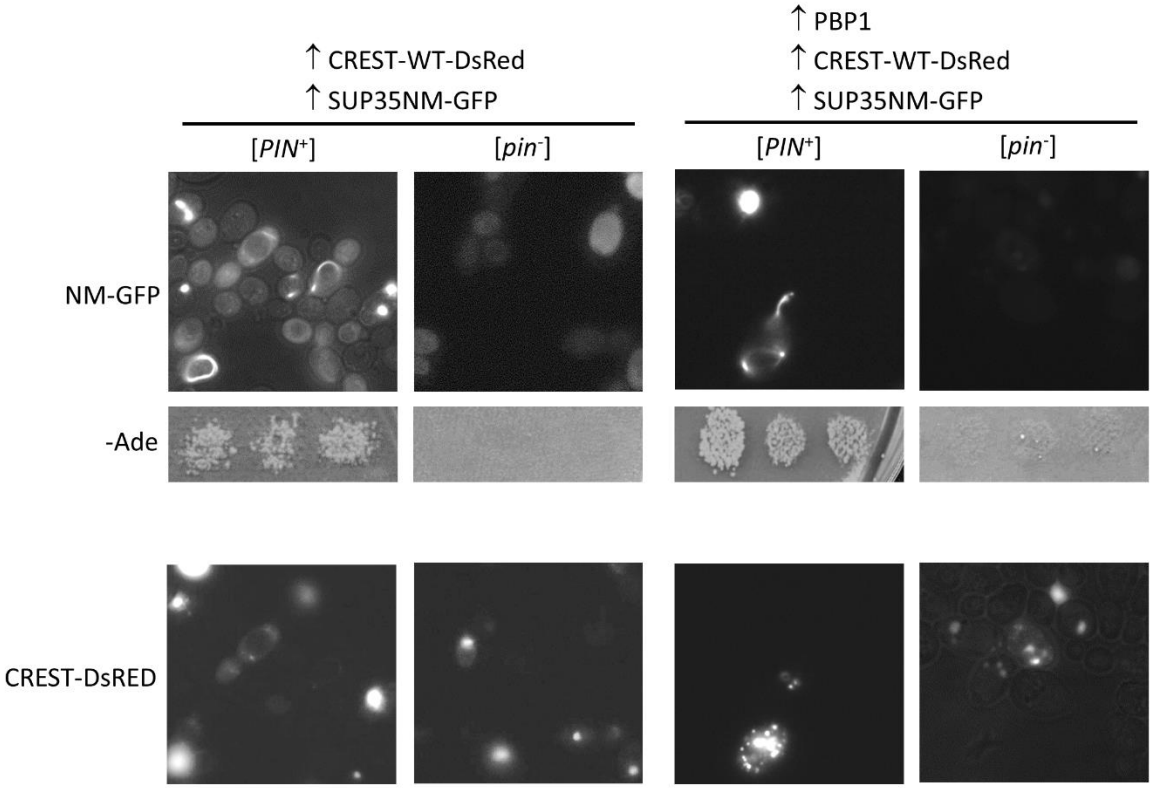

Figure S2. CREST does not facilitate induction of [*PSI*$^+$]. Isogenic [*PIN*$^+$] and [*pin*$^-$] 74D-694 strains transformed with plasmids YEp*GAL-CREST-DsRED* (↑CREST-DsRED) and *CUP1-SUP35NM-GFP* (↑SUP35NM-GFP) and YCp*GAL-PBP1-EGFP* (↑PBP1) were patched on plasmid selective SGal plates with 50 μM $CuSO_4$ and grown overnight. Cells were then examined under a fluorescent microscope with a GFP filter (upper) or mCherry filter (lower) and replica-plated onto medium lacking adenine (-Ade) where only [*PSI*$^+$] cells can grow. Plates were photographed after incubation. Patches of three independent transformants of [*PIN*$^+$] and [*pin*$^-$] are shown (middle).